

Electronic Structure of Rare-Earth Metals. I. Relativistic Augmented-Plane-Wave Calculations*

S. C. KEETON† AND T. L. LOUCKS‡

Institute for Atomic Research and Department of Physics, Iowa State University, Ames, Iowa 50010

(Received 26 October 1967)

Relativistic augmented-plane-wave calculations for Gd, Dy, Er, and Lu are reported. Energy bands, histograms of the density of states, and Fermi-surface cross sections are given. The Fermi surfaces of Dy, Er, and Lu are found to be quite similar to the one given earlier for yttrium. The Fermi surface of Gd is found to differ from the others by the absence of a "webbing" feature. Nesting between the sheets of the webbing is correlated with the occurrence of periodic moment arrangements in Dy, Er, and alloys of Y and of Lu with certain magnetic rare earths.

INTRODUCTION

THE first discussion of the relationship between itinerant electron antiferromagnetism and the Fermi-surface topography in multiband metals was given by Lomer.¹ He pointed out that the ordered magnetic moment in Cr is induced by exchange coupling between states on parallel portions of electron and hole surfaces. The resulting spin density wave (SDW) is characterized by a wave vector \mathbf{Q} equal to the separation between the parallel portions of the Fermi surface. The effect of the exchange interaction is to remove these portions of the Fermi surface, thus affecting the various transport phenomena. In Cr the vector \mathbf{Q} is determined by parallel regions on the hole "octahedron" and the body of the electron "jack." A semiquantitative verification of the relationship between the \mathbf{Q} vector and the Fermi surface has been provided by neutron-diffraction measurements,² while Zuckerman and Falicov³ have discussed the modifications of the Fermi surface on magnetic ordering.

The first suggestions that the rare-earth Fermi surfaces would be modified by the introduction of a SDW were given by Mackintosh⁴ and Miwa.⁵ Quantitative calculations^{6,6} were made on the nearly-free-electron model, which was the only one available at the time. Later, however, the augmented-plane-wave (APW) calculations of Dimmock and Freeman⁷ showed that the Fermi surface of Gd is extremely anisotropic and characterized by nearly flat regions perpendicular to

the c axis. Freeman *et al.*⁸ also reported APW calculations for Tm which were nearly the same as those for Gd, and they proposed that a substantial proportion of the resistivity anomalies well below the Néel point is due to the occurrence of higher-order superzone boundaries. At about the same time Williams *et al.*⁹ proposed a mechanism for antiferromagnetism in the rare earths similar to the one proposed by Lomer¹ for Cr but based on the exchange interaction between the localized $4f$ electrons and the itinerant electrons. They stressed that the significant feature of the Fermi surfaces must be the existence of regions in which hole and electron surfaces are parallel. The relationship between these parallel surfaces and the superzone boundaries was not of primary importance in this hypothesis, and the resistivity anomaly was considered to be due primarily to the annihilation of the electron and hole surfaces on ordering.¹⁰

To investigate further these possibilities we decided to perform detailed calculations of the Fermi surfaces of Gd, Dy, Er, and Lu. These elements are representative of the heavy rare earths and any trends in the band structures across the rare-earth series should become evident from a study of these four metals. It was apparent from preliminary investigations¹¹ that the calcu-

TABLE I. Lattice constants and atomic numbers Z for some rare-earth metals (a.u. = atomic units).

Metal	a (a.u.)	c (a.u.)	Z
Gd	6.871	10.93	64
Dy	6.784	10.67	66
Er	6.725	10.56	68
Lu	6.620	10.49	71

* Work was performed in the Ames Laboratory of the U. S. Atomic Energy Commission. Contribution No. 2176.

† Present address: Battelle Memorial Institute, Richland, Wash.

‡ Alfred P. Sloan Research Fellow.

¹ W. M. Lomer, Proc. Phys. Soc. (London) **80**, 489 (1962). A more recent discussion of this topic has been given by P. A. Fedders and P. C. Martin, Phys. Rev. **143**, 245 (1966).

² W. C. Koehler, R. M. Moon, A. L. Trego, and A. R. Mackintosh, Phys. Rev. **151**, 505 (1966).

³ M. J. Zuckerman and L. M. Falicov, in *Proceedings of the Tenth International Conference on Low-Temperature Physics, Moscow, 1966* (VINITI, Moscow, 1967).

⁴ A. R. Mackintosh, Phys. Rev. Letters **9**, 90 (1962).

⁵ H. Miwa, Progr. Theoret. Phys. (Kyoto) **29**, 477 (1963).

⁶ R. J. Elliot and F. A. Wedgwood, Proc. Phys. Soc. (London) **81**, 846 (1963).

⁷ J. O. Dimmock and A. J. Freeman, Phys. Rev. Letters **13**, 750 (1964).

⁸ A. J. Freeman, J. O. Dimmock, and R. E. Watson, Phys. Rev. Letters **16**, 94 (1966); and (to be published).

⁹ R. W. Williams, T. L. Loucks, and A. R. Mackintosh, Phys. Rev. Letters **16**, 168 (1966).

¹⁰ In a theoretical paper by Roth *et al.* [L. M. Roth, H. J. Zeiger, and T. A. Kaplan, Phys. Rev. **149**, 519 (1966)] the indirect exchange interaction is studied for arbitrary Fermi surfaces. They find results similar to those suggested by Lomer (Ref. 1) for Cr, i.e., nesting Fermi surfaces result in a long-range exchange interaction, the Fourier transform of which is peaked in the vicinity of a particular value of the wave vector.

¹¹ S. C. Keeton and T. L. Loucks, Phys. Rev. **146**, 429 (1966).

lations should be done relativistically¹² since we are interested in fairly subtle features of the Fermi surface which might be sensitive to these effects.

PROCEDURE

The crystal structure of the metals under consideration is hexagonal close packed. The lattice constants are listed in Table I. The crystal potential was approximated by a "muffin-tin" potential constructed using the method suggested by Mattheiss.¹³ The atomic charge densities used in constructing these potentials were obtained from the relativistic self-consistent-field calculations of Waber *et al.*¹⁴ Exchange was treated throughout using the Slater $\rho^{1/3}$ approximation. The APW sphere radii used for the various metals are listed in Table II. A complete discussion of the techniques involved in these RAPW calculations can be found elsewhere.¹⁵

The elements Dy and Er have free-atom configurations $4f^{10}6d^2$ and $4f^{12}6s^2$, respectively. In the metallic form, however, there are three conduction electrons (exhibiting some *d*-like character) and one less $4f$ electron than in the atomic state. There is therefore some question as to which is the most appropriate atomic configuration for use in constructing the muffin-tin potential. In order to determine the effect this might have on our final results, two potentials were used for both Dy and Er. For Dy the two potentials were constructed using charge densities for atomic configurations $4f^95d^16s^2$ and $4f^{10}6s^2$, and are denoted Dy 1 and Dy 2, respectively. For Er the two potentials were constructed using atomic configurations $4f^{11}5d^16s^2$ and $4f^{12}6s^2$, and are denoted Er 1 and Er 2, respectively. For the elements Gd and Lu the free-atom configurations $4f^75d^16s^2$ and $4f^{14}5d^16s^2$, respectively, were used in constructing the muffin-tin potential.

The energy bands for Dy 2 were calculated using 28 reciprocal lattice vectors. In all of the density-of-states and Fermi-surface calculations this basis set was extended to 32 reciprocal lattice vectors to ensure better

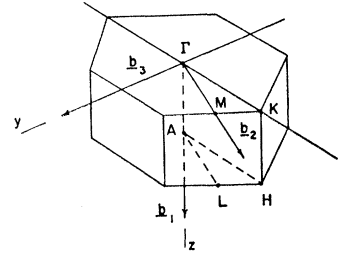


FIG. 1. Lower half of primitive Brillouin zone for the hexagonal close-packed crystal structure with the $1/24$ zone outlined by points of high symmetry.

convergence; these vectors are listed in Table III. The notation used is

$$(lmn) = \frac{2\pi}{a} \left(l\mathbf{i} + \frac{m}{\sqrt{3}}\mathbf{j} + \frac{na}{c}\mathbf{k} \right),$$

where \mathbf{i} , \mathbf{j} , \mathbf{k} are unit vectors along the x , y , z axes, respectively. The eigenvalues at all the symmetry points in the Brillouin zone (Fig. 1) were converged to within about 0.005 Ry using this basis set. The sum on K was truncated at -10 for the negative part and $+9$ for the positive. This means that orbital symmetries from $l=0$ to 9 were included in the calculations.

The calculations were carried out on a discrete mesh which is equivalent to 1200 points in the primitive Brillouin zone. The eigenvalues were calculated at 60 points in the $1/24$ zone, 15 points on each of the four levels designated 1, 3, 5, and 7 in Fig. 2. In order to get a larger sampling of the energy eigenvalues for the density-of-states calculation a more dense mesh was introduced. The 15 eigenvalues (circled in Fig. 2) on the levels designated 2, 4, and 6 were found by a second-order interpolation scheme. Additional energies within each of the levels were found in a similar manner. The resulting mesh is equivalent to 13 608 points in the primitive Brillouin zone.

RESULTS

The energy bands for all the elements studied are quite similar, differing only in details. We have therefore presented only our results for Dy 2. The differences in the energy bands near the Fermi energy for the various metals can be deduced from the Fermi surfaces, but for more complete results the reader is referred to the thesis on which this paper is based.¹⁶

Histograms on the density of states for each of the metals are shown in Fig. 3. The dotted curves on these figures represent the integrated density of states, with units given to the right. The Fermi energies are listed in Table II along with the corresponding value of the energy at the bottom of the band. The density of states

TABLE II. APW sphere radii R , Fermi energy E_f , energy at the bottom of the band E_0 , and the density of states at the Fermi energy $N(E_f)$.

Metal	R (a.u.)	E_f (Ry)	E_0 (Ry)	$N(E_f)$ (states/Ry atom)
Gd	3.32	0.425	0.082	28.5
Dy 1	3.16	0.450	0.075	27.7
Dy 2	3.32	0.505	0.104	24.3
Er 1	3.16	0.452	0.053	24.3
Er 2	3.16	0.519	0.091	23.6
Lu	3.16	0.453	0.018	25.5

¹² T. L. Loucks, Phys. Rev. **139**, A1333 (1965).

¹³ L. F. Mattheiss, Phys. Rev. **133**, A1399 (1964).

¹⁴ D. Liberman, J. T. Waber, and D. T. Cromer, Phys. Rev. **137**, A27 (1965).

¹⁵ T. L. Loucks, *Augmented Plane Wave Method* (W. A. Benjamin, Inc., New York, 1967).

¹⁶ S. C. Keeton, Ph.D. thesis, Iowa State University, Ames, Iowa, 1966 (unpublished).

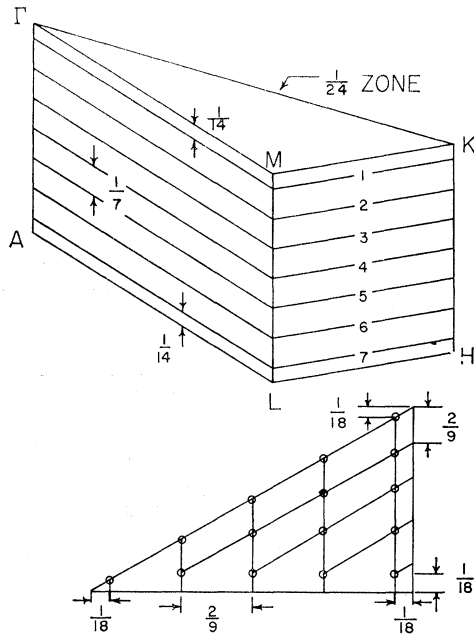


FIG. 2. $1/24$ zone showing the calculation mesh.

at the Fermi energy as determined from Fig. 3 is also listed in this table.

The intersections of the Fermi surface with the symmetry planes of the Brillouin zone for the metals studied are shown in Fig. 4. The intersections of the Fermi surface with the planes denoted by numbers 1-7 in Fig. 2 are shown in Fig. 5.

DISCUSSION

It is very difficult to visualize the rare-earth Fermi surfaces from the cross sections shown in Fig. 4. At first glance they all appear to be essentially the same, but there are differences across the series which are significant. Let us begin by looking at the Gd Fermi surface [Fig. 4(a)]. It is characterized by an electron surface which does not enclose the symmetry point M but pushes around L , thus pinching off the hole surface

TABLE III. Reciprocal lattice vectors \mathbf{K}_i used in the RAPW expansion based on $\mathbf{k}_i = \mathbf{k} - \mathbf{K}_i$ for all the points in the zone.

(000)	(001)	(110)
(001)	(111)	(110)
(111)	(111)	(111)
(002)	(020)	(021)
(112)	(110)	(020)
(110)	(112)	(021)
(111)	(021)	(111)
(002)	(111)	(021)
(111)	(200)	(201)
(022)	(112)	(112)
(201)	(003)	

TABLE IV. Comparison of the magnetic wave vector (in units of π/c) as determined from experiment (Refs. 18 and 19) and from the minimum separation of the webbing on the Fermi surfaces.

Metal	Y	Lu	Er	Dy	Gd
Experiment	0.54	0.53	0.57	0.49	0
Theory	0.49	0.45	0.54	0.46	0

along ALH . In the double-zone representation this Fermi surface looks very much like the one for Tm shown pictorially by Freeman *et al.*⁸ We do not agree with these authors that this is the Fermi surface of Tm; we have found that it is the result for Gd, and as we discuss later the Fermi surface of the heavier rare earths differs significantly from this model. The origin of the difference in our results from those of Freeman *et al.*⁸ is undoubtedly due to relativistic effects which we have shown earlier to be very important.¹¹ Ordinary APW calculations tend to produce this Gd-type Fermi surface for all of the heavy rare earths (see also the APW Fermi surface for Ho⁹). Our relativistic calculations yield results for Dy, Er, and Lu which are significantly different from Gd. Since Tm is between Er and Lu in the periodic table we expect it to have nearly the same Fermi surface as these two metals and hence different from Gd. But if it is not too confusing we can use the pictorial representation of the Fermi surface given by Freeman *et al.*⁸ while remembering that according to our calculation it is the Fermi surface for Gd instead of Tm.

For comparison let us now examine the Fermi surface of Lu [Fig. 4(f)] which is at the other end of the series of metals studied. In contrast to the result for Gd the electron surface now encloses the point M and the hole surface extends past AL almost to H . This yields a Fermi surface closely resembling the one given earlier for yttrium.¹⁷ In Fig. 5 of the yttrium paper¹⁷ the lower portion of the hole surface is shown in the double-zone representation. It is interesting to contrast this with our Gd Fermi surface. We see that the Gd Fermi surface has one arm at M and two others near L . If the arm at M is removed and the region between the two arms at L is filled with a "webbing," the Fermi surface becomes the yttrium type. We can summarize the differences between the two types of Fermi surfaces as follows: The Gd type has an arm at M , whereas the Y type has "webbing" between the two arms near L . We have found that Lu, Er 1, Er 2, and Dy 2 have the Y-type Fermi surface. Dy 1 is essentially Y-type except that in addition to the "webbing" there is also a small arm at M . Thus Dy is apparently transitory between the two types but definitely favoring the Y type.

These differences in Fermi surfaces depend on the relative positions of the fourth band at M and the third and fourth bands (which form a doubly degenerate

¹⁷ T. L. Loucks, Phys. Rev. **144**, 504 (1966).

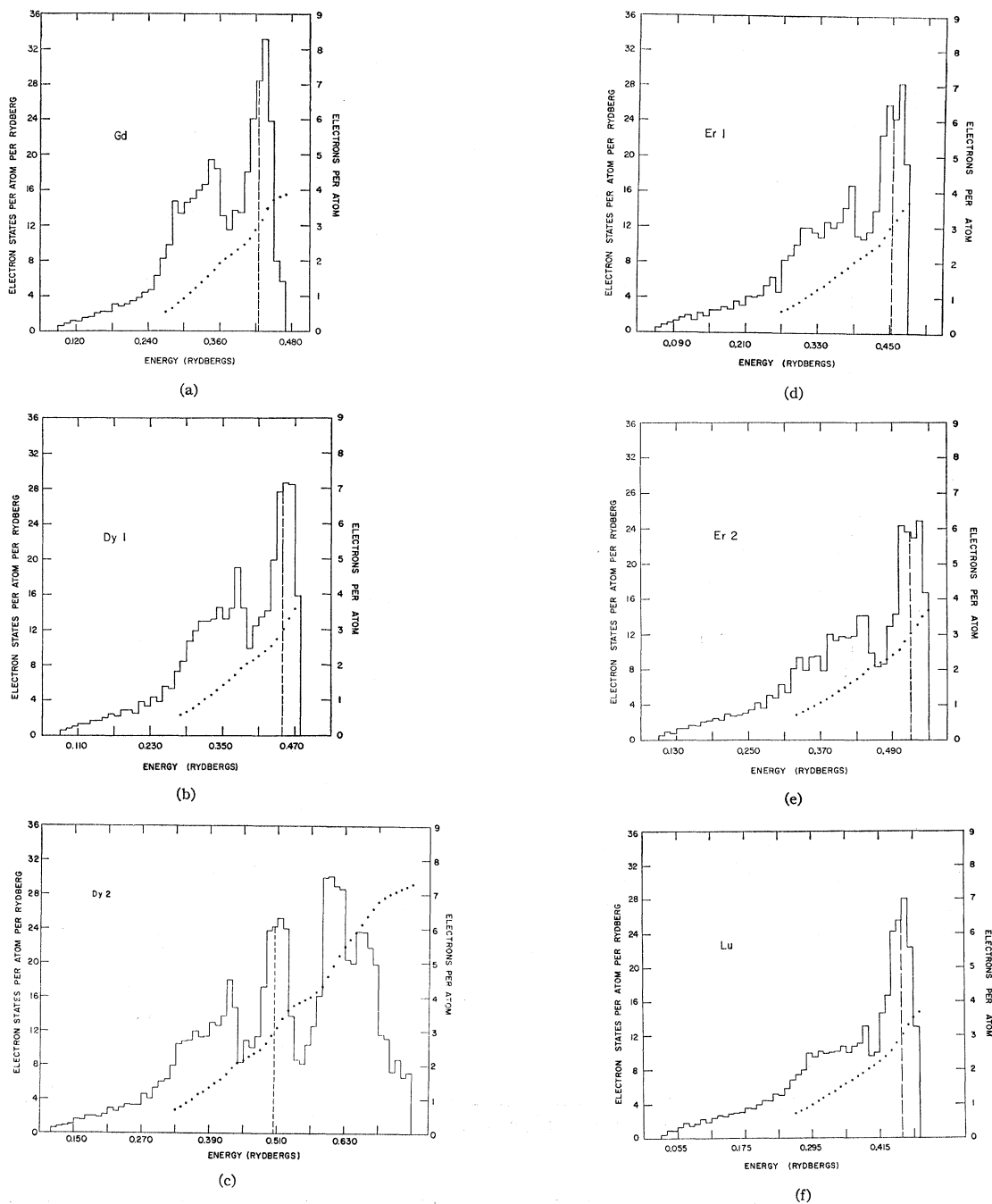


Fig. 3. Histograms of the density of states with the Fermi energy indicated by a dashed line. The dotted curve represents the integrated density of states, with the units given to the right. (a) Gd; (b) Dy 1; (c) Dy 2; (d) Er 1; (e) Er 2; (f) Lu.

level) at L . These levels have nearly the same energies and are either slightly above or slightly below the Fermi energy (Fig. 6). Because these bands are very flat their relative positions could be very sensitive to changes in the potential. One might wonder, therefore, if our *ad hoc* potentials are really good enough to yield accurate results. Probably not. But we do notice that

the two different potentials for Er both yield essentially the same Fermi surface, i.e., the Y type. Also the two potentials for Dy result in "webbing," although the presence of a small arm at M for one potential indicates that Dy is near the transition between the two types of Fermi surfaces. Although we might not have expected the potentials to be all that good, they have nevertheless

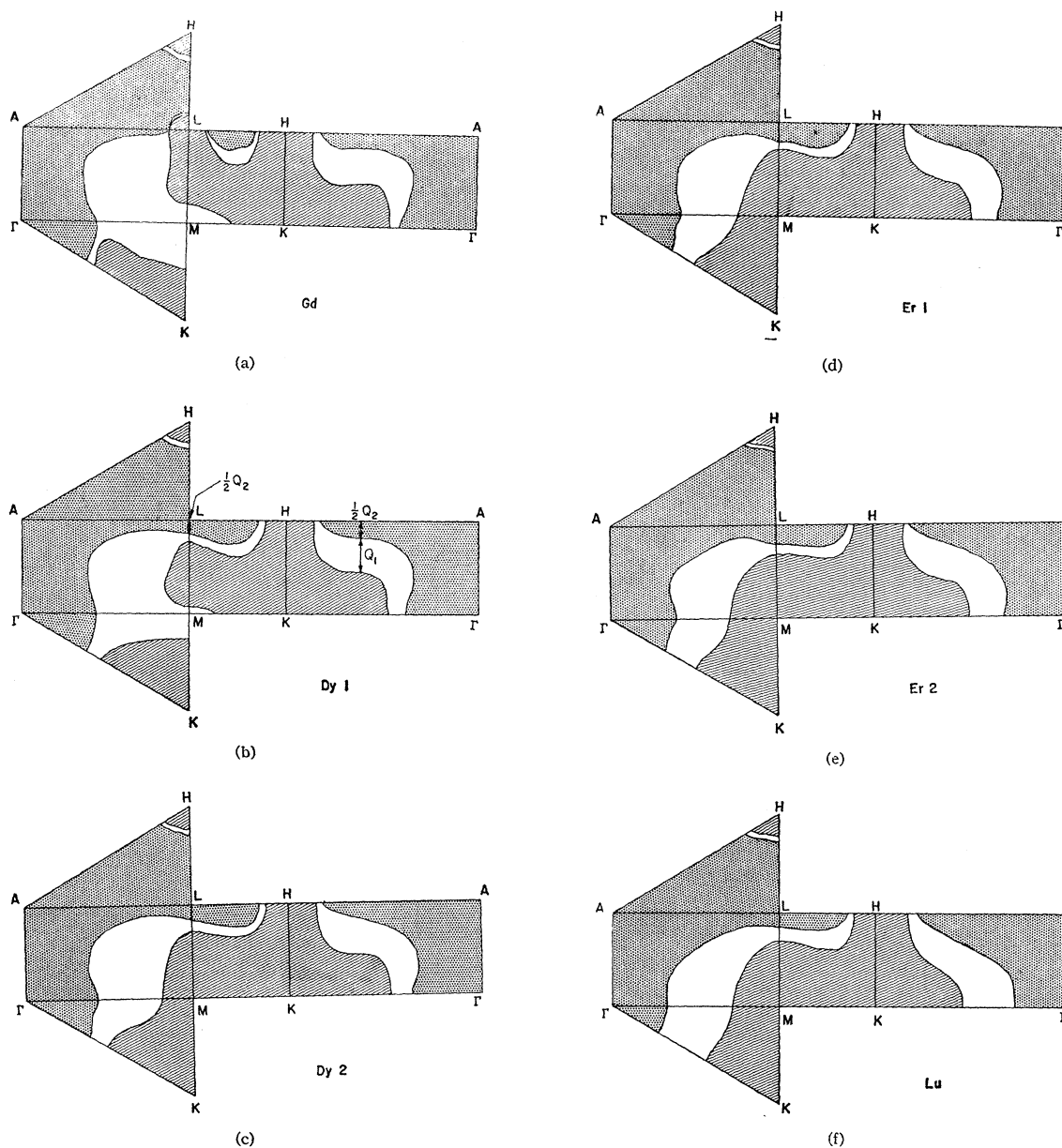


FIG. 4. Intersections of the Fermi surface with the symmetry planes of the Brillouin zone. The holes are shown dotted, the electrons lined. (a) Gd; (b) Dy 1; (c) Dy 2; (d) Er 1; (e) Er 2; (f) Lu.

yielded results from which we can deduce meaningful trends.

Returning now to the Fermi surface results, we can probably predict what the Fermi surface of Tb is like. Interpolating between the results for Gd and Dy 1, we would guess that Tb has an arm at M (intermediate in size) and that the "webbing" still exists between the arms at L but is probably much thinner than for Dy. In order to compare these features of the various Fermi surfaces we have shown the intersections with the $LMKH$ faces for the double-zone representation in

Fig. 7. The decrease in the "webbing" and the development of the arm at M can be seen in this figure.

The transition between the Y-type and the Gd-type Fermi surfaces correlates very nicely with various experimental results. First we notice that the Fermi-surface cross sections perpendicular to the c axis are different for the two types of Fermi surfaces (Fig. 5). This can result in different positron annihilation results as is very completely discussed in the companion paper by Williams and Mackintosh. In addition we notice a correlation between the webbing and the occurrence of

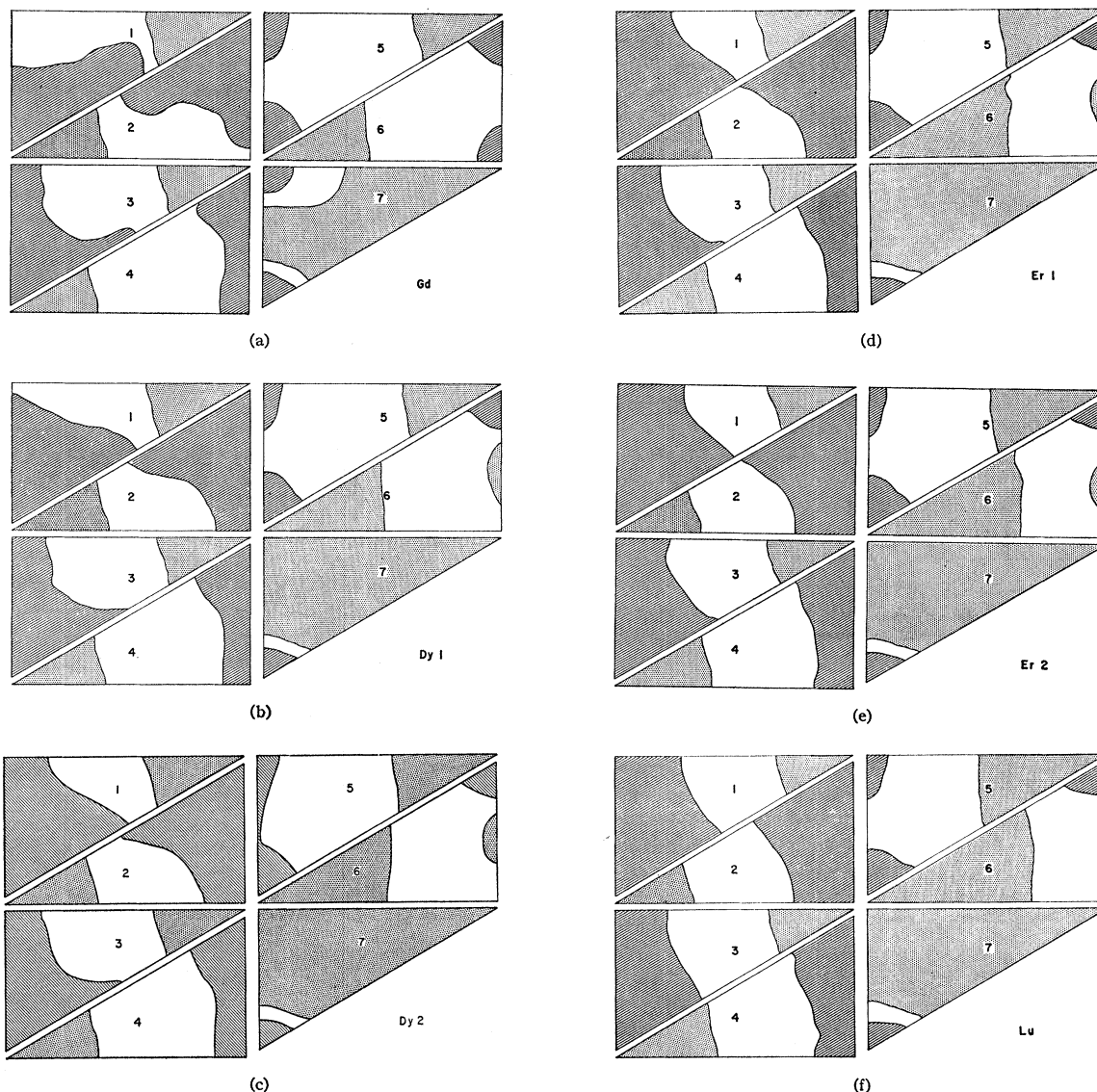


FIG. 5. Intersections of the Fermi surface with the planes denoted 1-7 in Fig. 2. The holes are shown dotted, the electrons lined. (a) Gd; (b) Dy 1; (c) Dy 2; (d) Er 1; (e) Er 2; (f) Lu.

periodic moment arrangements in some of the heavy rare earths and certain alloys of Y and Lu with magnetic rare earths (Sc also falls in this latter category, but these results will be published separately). In Fig. 7 we have also shown the experimentally determined values of the magnetic wave vector Q for each of the metals.^{18,19} The correlation between the thickness of the webbing and the magnetic Q vector is very good. The numerical values for the *minimum* thickness of the webbing are given in Table IV along with the experimental Q vectors (probably some average thickness

¹⁸ W. C. Koehler, J. Appl. Phys. 36, 1078 (1965).

¹⁹ H. E. Nigh, S. Legvold, F. H. Spedding, and B. J. Beaudry, J. Chem. Phys. 41, 3799 (1964).

should be used and this would improve the agreement with experiment, but for the present purposes the minimum thickness is adequate). The rather remarkable agreement shown in this table is a good indication that the webbing feature of the Fermi surface is responsible for the occurrence of periodic moment arrangements in these metals. The absence of the webbing in Gd implies that it should order ferromagnetically, which indeed it does. We notice also that the unusually small Q vector for Tb is consistent with the view that the webbing for this metal is probably thinner (Fig. 7).

It is also significant with respect to the positron annihilation results discussed in the companion paper that below the ordering temperature the magnetic gaps

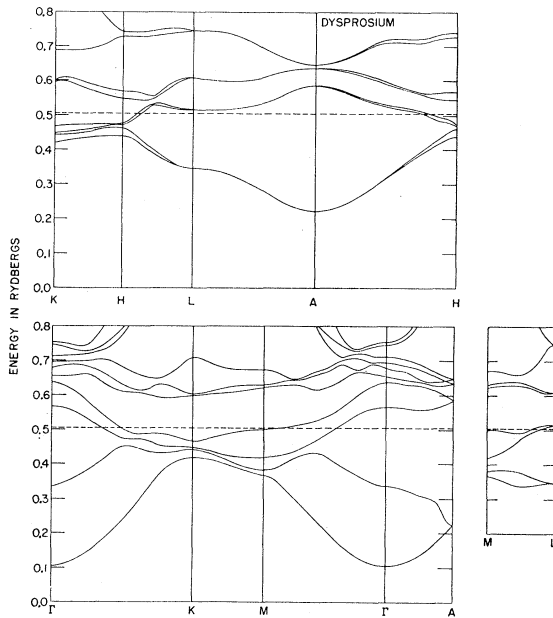


FIG. 6. Energy bands for Dy 2 along the symmetry axes of the Brillouin zone. The dashed line indicates the Fermi energy.

remove the webbing in the Y-type Fermi surfaces thus making them quite similar to the Gd type. The corresponding decrease in Fermi-surface area perpendicular to the c axis presumably results in the observed increase in the resistivity near the ordering temperature.

That nesting between the two sheets of the webbing is associated with the periodic moment arrangements in the heavy rare earths and certain alloys is a new suggestion. Previous calculations for Tm by Freeman *et al.*⁸ could not have yielded this possibility because their nonrelativistic results did not have the webbing feature. As discussed above the nonrelativistic calculations for heavy rare earths have resulted in Gd-type Fermi surfaces. Freeman *et al.*⁸ have shown that even the Gd-type Fermi surface has some points separated by the mag-

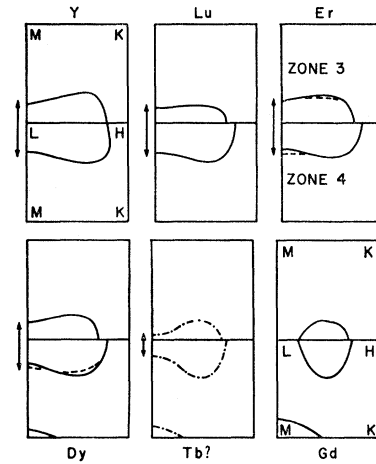


FIG. 7. Cross sections of various Fermi surfaces showing webbing feature.

netic Q vector, but we feel that not enough states are involved unless the webbing feature is also present, thus excluding the possibility of Gd having a periodic moment arrangement.

Our nesting feature is also different from the one proposed by Williams *et al.*⁹ They suggested that nesting between nearly parallel portions of electron and hole surfaces *in the reduced zone* were responsible for the periodic moment arrangements. It has been pointed out, however, that this form of nesting is not important because it involves coupling between two occupied regions of the Brillouin zone.²⁰

ACKNOWLEDGMENTS

Both of the authors are very grateful to A. R. Mackintosh for close collaboration during this project, and one of them (T.L.L.) is deeply indebted for the gracious Danish hospitality extended to him during a recent visit to The Technical University at Lyngby.

²⁰ W. M. Lomer (private communication).